

# Random-Orientation High-Spin Electron Spin Resonance Spectroscopy and Comprehensive Spectral Analyses of the Quintet Dicarbene and Dinitrene with *meta*-Topological Linkers: Origins of Peculiar Line-Broadening in Fine-Structure ESR Spectra in Organic Rigid Glasses

Teruaki Koto,<sup>†</sup> Kazunobu Sato,<sup>\*,†</sup> Daisuke Shiomi,<sup>†</sup> Kazuo Toyota,<sup>†</sup> Koichi Itoh,<sup>†,‡</sup> Edel Wasserman,<sup>§</sup> and Takeji Takui<sup>\*,†</sup>

Departments of Chemistry and Materials Science, Graduate School of Science, Osaka City University, Sumiyosi-ku, Osaka 558-8585, Japan, and Du Pont Central Research & Development, Wilmington, Delaware 19880-0328

Received: May 7, 2009

In high-spin chemistry, random-orientation fine-structure (FS) electron spin resonance (ESR) spectroscopy entails advantages as the most facile and convenient method to identify high-spin systems, as frequently reported in the literature. Random-orientation ESR spectroscopy applicable to organic high-spin entities can date back to the Wasserman and co-workers' attempt on the first spin-quintet dicarbene, *m*-phenylenebis(phenylmethylene) (*m*-PBPM), in the 2-MTHF glass in 1963 and 1967, following their successful work on randomly oriented triplet-state ESR spectroscopy. The FS ESR spectrum of *m*-PBPM in the 2-MTHF glass, however, has never fully been analyzed due to a peculiar line-broadening appearing at many canonical peaks. Organic high-spin spectra from most quintet dinitrenes also suffer from similar phenomena. Seemingly intrinsic line-diffusing or -broadening phenomena adversely affect the reliable determination of FS parameters for organic high-spin entities in rigid glasses. In high-spin chemistry, the line-broadening has been an obstacle that masks key FS transitions in many cases. Thus, both the origin of the broadening and the comprehensive spectral analysis have been a long-standing issue. In this report, we examine the origin of the line-broadening appearing in the FS ESR spectra, illustrated by a comprehensive spectral analysis for *m*-PBPM in the quintet ground state and the first-documented quintet-state dinitrene, *m*-phenylenebis(nitrene) (*m*-PBN) in the 2-MTHF glass. A complete analysis of the random-orientation FS spectra from *m*-PBPM diluted in the benzophenone crystal has shown that the *g*-anisotropy of *m*-PBPM is not prominent. Also the higher-order FS terms such as  $S_i^2 S_j^2$  group-theoretically allowed for  $S = 2$  are not necessary in spite of the argument for a hydrocarbon-based tetraradical ( $S = 2$ ) in the ground state. Our new approach to the line-broadening analysis invokes both exact analytical solutions for the resonance fields of canonical peaks and the magnetic-parameters gradient method. The *D*- and *E*-values of *m*-PBPM acquired by the spectral simulation in this study give different molecular structures of the quintet dicarbene in the benzophenone crystal lattice ( $D = +0.0703_0 \text{ cm}^{-1}$ ,  $E = +0.0212_0 \text{ cm}^{-1}$ ) and in the 2-MTHF glass ( $D = +0.0780_0 \text{ cm}^{-1}$ ,  $E = +0.0221_0 \text{ cm}^{-1}$ ). Microscopic origins of the line-broadening observed for high-spin oligocarbenes or oligonitrenes generated by photolysis in organic glasses have been proposed.

## Introduction

High-spin chemistry has underlain the continuing development of molecule-based magnetism as an interdisciplinary field in pure and applied sciences.<sup>1</sup> The first organic spin-quintet entity, *m*-phenylenebis(phenylmethylene) (abbreviated to *m*-PBPM) in the ground state, whose molecular design is based on the topological symmetry argument of  $\pi$ -electron network in alternant hydrocarbons,<sup>1,2a</sup> can date back to the report by Itoh<sup>2a</sup> and the one by Wasserman<sup>2b</sup> et al. in 1967. The former was carried out by a single-crystal electron spin resonance (ESR) and the latter by random-orientation ESR spectroscopy in an organic rigid glass, respectively. The latter has been a particularly facile and convenient method to identify high-spin sys-

tems.<sup>1</sup> In terms of random-orientation spectroscopy, the latter was the first attempt to experimentally derive fine-structure (FS) parameters from organic high-spin entities by invoking computer-spectral simulation, following the successful work on randomly oriented triplet-state ESR spectroscopy.<sup>3</sup> With the first quintet hydrocarbon, *m*-PBPM, however, the FS ESR spectrum observed in the 2-MTHF glass has never fully been analyzed due to peculiar line-broadening appearing at many canonical peaks. Organic high-spin spectra from quintet dinitrenes also suffer from similar phenomena.<sup>4</sup> Seemingly intrinsic line-diffusing or -broadening phenomena hinder random-orientation ESR spectroscopy for the reliable determination of FS parameters of organic high-spin entities in rigid glasses.

Indeed, in high-spin chemistry the line broadening has been an obstacle that masks key FS transitions in many cases of organic high spins except for quartet hydrocarbons.<sup>5b</sup> Thus, both the FS spectral analysis of *m*-PBPM as a typical organic quintet species and the origin of the broadening relevant to the

\* Corresponding authors. E-mail: K.S., sato@sci.osaka-cu.ac.jp; T.T., takui@sci.osaka-cu.ac.jp.

<sup>†</sup> Osaka City University.

<sup>‡</sup> Deceased on June 26, 2008.

<sup>§</sup> Du Pont Central Research & Development.

comprehensive spectral analysis have been a long-standing issue. In this report, we examine the origin of the line-broadening appearing in the FS ESR spectra from organic high spins in rigid glasses, illustrating the comprehensive spectral analysis for the first spin-quintet dicarbene, *m*-PBPM, and dinitrene, *m*-phenylenebis(nitrene) (*m*-PBN), in the 2-MTHF glass. Our approach to the line-broadening analysis invokes both exact analytical solutions for the resonance fields of canonical peaks<sup>6</sup> and a magnetic-parameters gradient method: Both the analytical expressions and the gradient method developed in our laboratory (Osaka City University) can be applicable to any physical systems with high-spin multiplicities if their fine-structure spin Hamiltonians do not include higher-order terms such as  $S_i^2 S_j^2$ , which are usually omitted for chemical entities with small spin-orbit couplings. The quintet hydrocarbon, *m*-PBPM, in this work provides a testing ground for this issue, as its complete FS spectral analysis is obtained for the randomly oriented *m*-PBPM systems. In the original work by both Itoh and Wasserman et al., the higher-order terms were found not to be necessary for the FS spectral analysis of the quintet dicarbene<sup>2</sup> and dinitrene.<sup>2b</sup> Seemingly, our gradient method may have some similarity to strain effect analyses, which have been nicely incorporated in spectral simulation softwares such as EasySpin.<sup>7a</sup> In the conventional strain effect analyses,<sup>7</sup> the effects are treated as phenomenological parameters, but in the gradient method given in this study the FS-relevant line-broadening is described by analytical expressions derived from FS-relevant spin Hamiltonian terms. In this report, comprehensive analyses for FS ESR spectroscopy for randomly oriented high-spins are based on X-band CW ESR spectroscopy with both the conventional perpendicular and the parallel microwave excitations. The *D*- and *E*-values of *m*-PBPM acquired by the spectral simulation in this study give us the difference in the molecular structure of the quintet dicarbene, *m*-PBPM between the benzophenone crystal lattice and the 2-MTHF glass. A well-established semiempirical approach<sup>1,2,5</sup> has been applied to the calculation for the FS tensor of *m*-PBPM, in which the **D** tensor for oligocarbenes or oligonitrenes are assumed to be built up by the component  $D_i$  tensors of monocarbenes or mononitrenes. Microscopic origins for the line-broadening appearing in the quintet FS spectra of *m*-PBPM and *m*-PBN are proposed, on the basis of their molecular structural variation in the 2-MTHF frozen glasses.

## Methods of Comprehensive Analysis

**1. Exact Analytical Solutions for Fine-Structure Canonical Resonance Fields of a Quintet State.** In our approach, we have fully utilized the exact analytical expressions<sup>6</sup> for the FS canonical resonance fields. These are derived from eigenfield equations<sup>8</sup> in the absence of the higher-order FS terms for  $S = 1, 2$ , as given in the Supporting Information (Table S1). The original eigenfield approach solves directly any resonance fields in field-swept magnetic resonance under fixed oscillating radio and/or microwave frequencies without solving eigenenergies associated with a spin Hamiltonian in the presence of the static magnetic field. The approach is powerful and is applicable to the spin Hamiltonians including the higher-order FS terms, but the corresponding analytical solutions are intractable for higher spin multiplicities.<sup>6</sup> The present gradient method utilizes only  $S_i S_j$  terms for the FS interactions. It has been found that the FS canonical exact resonance fields can analytically be solved up to  $S = 4$  while the analytical expressions for exact resonance fields in an arbitrary orientation of the static magnetic fields are obtained up to a quartet state.<sup>6</sup> The analytical expressions enable us to analytically derive the first derivatives (gradients

such as  $\partial B/\partial D$  and  $\partial B/\partial E$ ) of the canonical resonance fields (*B*) with respect to any spin Hamiltonian parameters, *g*, and *D*- and *E*-values. Practically, we have utilized Mathematica (MATLAB 6.5) for working with the extremely lengthy equations of targeted gradients. Thus, the gradient method proposed here is applicable to principal-off-axis extra peaks, but the exact analytical expressions for the off-axis extra lines are not mathematically available. Only expressions based on second-order perturbation treatments are available for an arbitrary spin quantum number.<sup>9</sup> For *m*-PBPM with relatively large FS parameters, the perturbation expressions are not suitable for the line-broadening analysis of the extra lines, because of the limitations of the perturbation approach at X-band ESR spectroscopy. The difference between other reported methods,<sup>7</sup> such as strain effects, and ours is that the gradient method is based on the determined spin Hamiltonian itself and does not require additional empirical variables to identify stationary points such as canonical or principal-off-axis extra lines. The only weakness of our analytical exact solutions is the lack of higher-order FS terms such as  $S_i^2 S_j^2$  in the spin Hamiltonian, which are usually omitted for high-spin entities characterized by small spin-orbit couplings but group-theoretically allowed for *S* larger than  $3/2$ . The importance of the higher-order terms has been pointed out for a neutral high-spin hydrocarbon observed in an organic glass in terms of the FS spectral simulation.<sup>10</sup> Thus, it is important whether such higher-order terms are really necessary for high-spin organic entities with small spin-orbit couplings. In this work, a high-spin hydrocarbon, *m*-PBPM, in its quintet state has been chosen, because the completely pulverized powder sample of *m*-PBPM magnetically diluted in diamagnetic crystal lattices can afford a randomly oriented ideal system of quintet hydrocarbons. The complete FS spectral simulation for the polycrystalline sample from *m*-PBPM diluted in a benzophenone single crystal<sup>2a</sup> has been carried out, illustrating that the higher-order FS terms are not necessary, as described below.

**2. Conventional Perpendicular- and Parallel-Excitation High-Spin ESR Spectroscopy for the Polycrystalline Sample of the Quintet Dicarbene, *m*-PBPM Magnetically Diluted in the Benzophenone Crystal.** We have revisited the “single-crystal” ESR study of *m*-PBPM magnetically diluted in the benzophenone crystal lattice<sup>2a</sup> to establish our comprehensive analysis of random-orientation FS spectroscopy for the polycrystalline (powdered) sample. The revisitation is meaningful to help understand the complexion appearing in the FS spectral features of *m*-PBPM in the frozen glass. We have carried out FS spectral measurements in both perpendicular (conventional) and parallel excitation modes of X-band microwave irradiation, completely analyzing the spectra by the hybrid eigenfield method developed in our laboratory.<sup>6</sup> Our hybrid eigenfield method utilizes the ordinary eigenenergy-solution approach for exact eigenfunctions to compute transition probabilities of all the FS transitions for the random orientation of high spins with respect to the static magnetic field. This bypass approach is achieved by diagonalizing the eigenenergy matrices with the exact eigenfields once they are acquired by diagonalizing the corresponding eigenfield matrices. The procedure greatly reduces CPU time and circumvents any difficulties in solving the eigenfunctions in generalized eigenvalue-eigenfunction problems.

The polycrystalline sample of *m*-PBPM is suitable for analyzing the FS line shapes in the wide range of the swept magnetic field. The line width of the single FS transition is subject to the contribution from proton hyperfine interactions, these being checked by the X-band single-crystal ESR spectroscopy prior to the polycrystalline ESR measurements. The

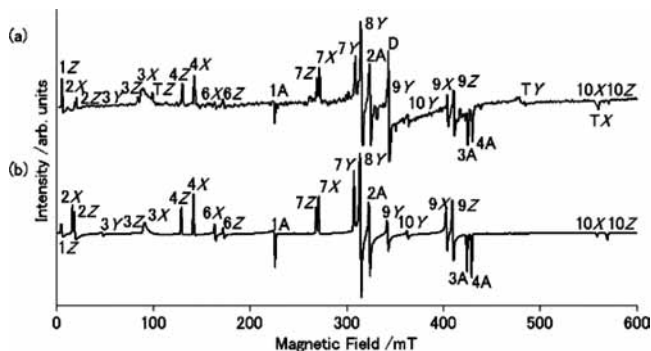


**Figure 1.** Random-orientation X-band FS ESR spectra of *m*-PBPM in the benzophenone lattice and transition assignments. The symbols have the same meanings as given in Figure 2. (a) Observed spectrum at 4.0 K. The experimental conditions were as follows: MW frequency, 9.634 642 2 GHz; MW power, 0.01 mW; modulation frequency, 100 kHz; modulation amplitude, 0.49 mT. The spectral assignments, X, Y, Z and A denote the canonical peaks and an off-principal-axis extra line, respectively. The symbols, X, Y, and Z correspond to the magnetic field orientation along the principal axis of the **D** tensor. The *m*-phenylene-based triplet species generated during the photolysis and the doublet peak (343.78 mT), which is an extremely stable byproduct generated during the sample preparation, are denoted by T and D, respectively. (b) Simulated spectrum. Spin Hamiltonian parameters used:  $S = 2$ ,  $D = +0.0703_0 \text{ cm}^{-1}$ ,  $E = +0.0212_0 \text{ cm}^{-1}$ ,  $g = 2.003$ , and line width 1.17 mT. Theoretically, 30 canonical peaks should be analytically obtained. In the perpendicular excitation spectrum, the number of the assignable canonical peaks was 27. 1Z, 1X, and 1Y with imaginary resonance fields are omitted.

line shape is Gaussian, as expected for the magnetically well-diluted sample. The complete sets of the FS spectral simulations for *m*-PBPM, including the angular dependences of resonance fields and transition intensities are given in the Supporting Information.

First, parts a and b of Figure 1 show the FS spectrum observed in the perpendicular excitation mode and the corresponding simulation with complete transition assignments, respectively. The assignments have been made by identifying stationary peaks (canonical and principal-off-axis lines<sup>9</sup>) with the help of the angular dependence of the FS resonance fields and transition intensities. All the spectral simulations with a single set of the  $g$ -value and FS parameters for the quintet and with one for the triplet species, i.e.,  $S = 2$ ,  $g = 2.003$  (isotropic),  $D = +0.0703_0 \text{ cm}^{-1}$ ,  $E = +0.0212_0 \text{ cm}^{-1}$  for *m*-PBPM, and  $S = 1$ ,  $g = 2.003$  (isotropic),  $D = +0.4167_6 \text{ cm}^{-1}$ ,  $E = +0.0201_5 \text{ cm}^{-1}$  for the phenylmethylene-based triplet species as the byproduct, have satisfactorily reproduced the observed spectra. There was neither occurrence of any particular line-broadening except for the hyperfine contributions from protons nor any molecular structural fluctuations of *m*-PBPM in the benzophenone lattice. We have noted that there is a subtle difference between the  $D$ - and  $E$ -values determined from the polycrystalline sample studied in this work and those previously reported;  $S = 2$ ,  $g = 2.003$ ,  $D = +0.07131 \text{ cm}^{-1}$ ,  $E = +0.01902 \text{ cm}^{-1}$ .<sup>2a</sup> These FS parameters previously reported have not reproduced in detail the observed polycrystalline FS spectrum shown in Figure 1. The spin Hamiltonian parameters for the single-crystal work were derived from the third-order perturbation theory based on the K-band (24 GHz) ESR measurements: The least-squares-fitting procedure was carried out in the second-order perturbation treatment<sup>2a</sup> and the rms assessment during the analysis was based on the comparison of the resonance fields with those calculated in the third order.<sup>11</sup> The experimental accuracy in setting the single crystal in the *abc* crystallographic axes reference frame was within  $0.3^\circ$ .<sup>11</sup> Thus, the difference found in this work can be

interpretable as an instrumental limitation in the single crystal work. We believe that the updated parameters found for the polycrystalline sample and by the hybrid eigenfield approach are more accurate, except for the molecular information on the principal axes of the **D** tensor.

The angular dependences of the resonance fields and transition intensities were calculated in terms of the hybrid eigenfield method with the spin Hamiltonian composed of an electron Zeeman and FS term of  $\mathbf{S} \cdot \mathbf{D} \cdot \mathbf{S}$ , completing the FS spectral assignments including off-principal axis transitions, as shown in Figure 1Sc (Supporting Information): The transition intensities include the Boltzmann factors for the magnetic sublevels. Notably, the complete analyses show that the  $g$ -anisotropy of *m*-PBPM is not prominent and that the higher-order FS terms group-theoretically allowed for  $S = 2$  are not necessary in spite of the argument for a hydrocarbon-based tetraradical ( $S = 2$ ) in the ground state.<sup>10</sup> The vanishing higher-order FS terms with the isotropic  $g$ -value is consistent with small spin-orbit interactions expected for *m*-PBPM as a hydrocarbon. The vanishing higher-order terms and the isotropic  $g$ -value are also consistent with the results from the single crystal work.<sup>2a</sup> To claim the necessity of the higher-order FS terms for high-spin hydrocarbons, in addition to complete spectral simulations some physical rationale is required such as nearby excited states interacting via spin-orbit couplings.

Parallel excitation experiments, as shown in Figure 2, and spectral assignments were carried out for the polycrystalline sample of *m*-PBPM for the first time. All the FS transitions observed in fields below 0.35 T are allowed in this detection scheme. Most of the “allowed transitions” appearing in the perpendicular excitation mode, as shown in Figure 1a, disappear in Figure 2a. The spin Hamiltonian parameters determined from the perpendicular excitation experiments satisfactorily reproduced the parallel excitation spectrum as shown in Figure 2b, illustrating that the parameters are accurate enough. In the parallel excitation experiments, we have used a dual-mode microwave resonator (Bruker BioSpin, 4116DM), which enables us to electronically switch the conventional perpendicular mode to the parallel excitation mode under the same sample and instrumental conditions. Only the  $Q$ -values and resonant frequencies were not the same. The parallel excitation spectroscopy is particularly powerful for distinguishing, in a straightforward manner, between doublet and high-spin species in their mixture.<sup>9</sup> Also, the parallel excitation spectroscopy is useful for identifying hyperfine forbidden transitions.<sup>12</sup>

**3. Magnetic Parameters Gradient Method in terms of Exact Analytical Resonance Fields for High Spins. 3.1. Gradient Method Applied to a Random-Orientation ESR Spectrum of *m*-PBPM in an Organic Glass.** The successful spectral analyses of *m*-PBPM in the polycrystalline state and the available exact analytical expressions of the resonance fields for  $S = 2$  without the higher-order terms such as  $S_i^2 S_j^2$  have encouraged us to fully analyze the quintet FS spectrum with a peculiar and notorious line-broadening observed in the 2-MTHF. Figure 3a shows an experimental FS spectrum of *m*-PBPM in its quintet ground state, observed in the 2-MTHF glass at 2.7 K after the photolysis of the corresponding diazo precursor at the same temperature. In sharp contrast to the spectrum in Figure 1a, a line-broadening is featured in many canonical and extra lines. Overall, the organic-rigid-glass FS spectrum looks simplified due to the broadening (masking), leading to the missing or blurring of key canonical lines. By invoking the exact analytical expressions,<sup>6</sup> we are able to compute the magnitudes of  $\partial B/\partial g$ ,  $\partial B/\partial D$ , and  $\partial B/\partial E$ , termed “on-resonance magnetic-parameters



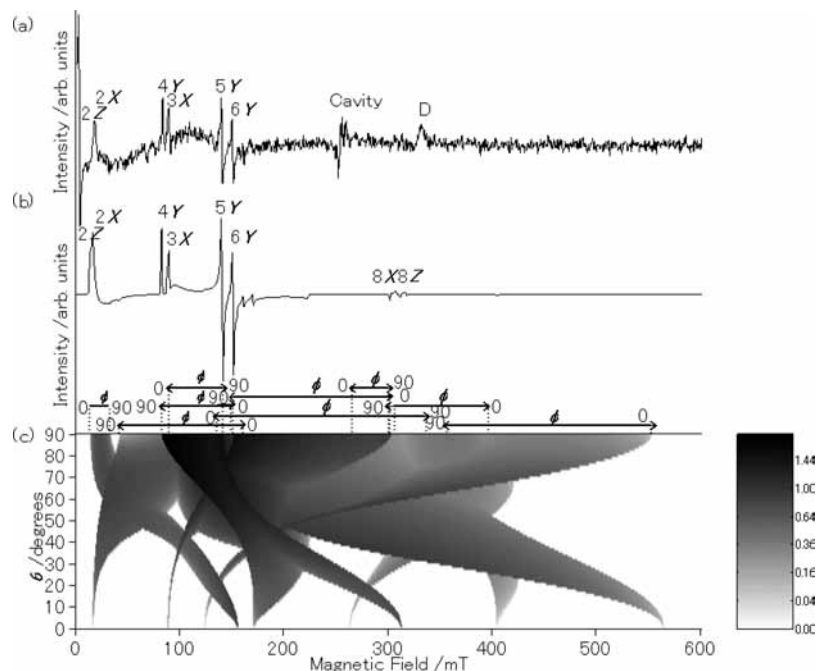


**Figure 2.** Random-orientation X-band FS ESR spectra of *m*-PBPM in the benzophenone crystal lattice and transition assignments with the help of the angular dependence of the resonance fields and transition intensities in the parallel microwave excitation mode. Instrumental details are in the following: (a) Observed spectrum at 4.0 K. The experimental conditions were as follows: MW frequency, 9.420 235 0 GHz; MW power, 0.1 mW; modulation frequency, 100 kHz; modulation amplitude, 0.49 mT. The symbols have the same meanings as in Figure 1a. (b) Simulated spectrum. Spin Hamiltonian parameters used:  $S = 2$ ,  $D = +0.0703_0 \text{ cm}^{-1}$ ,  $E = +0.0212_0 \text{ cm}^{-1}$ ,  $g = 2.003$ , line width 1.17 mT. (c) The symbols  $\theta$  and  $\phi$  denote the polar angles for defining the direction of the static magnetic field vector. The calculated transition intensities of all the resonance fields are depicted by light and shade drawing, relatively. The angular dependence of the resonance fields and transition intensities with the Boltzmann factors considered. All the resonance fields and transition probabilities have been calculated by a hybrid eigenfield method developed in our laboratory. A strong peak at the zero-field was due to the sudden start of the magnetic field sweep.

gradients". Figure 3b shows the simulated FS spectrum of *m*-PBPM in the 2-MTHF glass by the hybrid eigenfield method with a refined set of the spin Hamiltonian parameters:  $S = 2$ ,  $g = 2.003$  (isotropic),  $D = +0.0780_0 \text{ cm}^{-1}$ ,  $E = +0.0221_0 \text{ cm}^{-1}$ .<sup>13</sup> It is worth noting that the refined  $D$ -value is 11% greater than the documented one.<sup>2b,14</sup> Also, we have noted that a significant difference between the  $D$ -value derived from the frozen glass sample<sup>15</sup> and that from the polycrystalline sample. The difference arises from the molecular structure difference at the divalent carbon sites in the frozen glass and the benzophenone lattice, which gives more strained environments.<sup>2a</sup> The principal axes analysis based on the single crystal work indicated that *m*-PBPM replaces two benzophenone molecules in the unit cell (orthorhombic,  $Z = 4$ ).<sup>11</sup> A probable interpretation for the larger  $D$ -value will be given below in terms of the  $\mathbf{D}$  tensor calculation, in connection with the possible origin of the line-broadening.

Parallel microwave irradiation experiments were carried out to make "forbidden transitions" show up in the field lower than 200 mT (see Figure S4 in Supporting Information), good agreement between the observed and simulated spectra illustrating the accuracy of the experimentally derived magnetic parameters above.<sup>15</sup> It should be noted that in Figure 3 the agreement in terms of the resonance fields free from the line-broadening between experiment and theory was within the line width (1.17 mT) used for the single FS transition during the simulation.

As depicted by slanting sticks between (a) and (b) of Figure 3, we have computed the  $D$ - and  $E$ -value gradients for the canonical lines throughout the analyses. During the analysis, we have frequently employed the exact analytical expressions for the canonical FS resonance lines (see Table S1 in Supporting Information for the expressions). The larger slanting angles

designate the greater gradient effects, giving rise to prominent line-broadening, if the corresponding principal axes of the FS  $\mathbf{D}$  tensor undergo any spatial fluctuations or variations (we prefer the latter wording). The gradient effects are a measure that reflects molecular structural variations associated with the particular principal axes in the random-orientation FS spectroscopy in organic rigid glasses or frozen media such as argon matrices. In Figure 3a, the broad peaks denoted by 3Y, 4Z, 4X, 6X, and 6Z below 200 mT are characterized by at maximum 1 order of magnitude larger  $\partial B/\partial D$  and  $\partial B/\partial E$  compared with those of the other canonical peaks. Also, the peak 10X has large  $\partial B/\partial D$  and  $\partial B/\partial E$ . The peak 10Z at the highest field, which should be important as one of the key peaks, has large  $\partial B/\partial D$ , making it difficult to clearly be detected. The misassignment of this outermost canonical line gives a 10% smaller  $D$ -value than  $+0.0780 \text{ cm}^{-1}$ . All the computed values of the gradient effects are given in Table S2 in the Supporting Information, and how the gradients explicitly affect the FS rigid-glass spectra of *m*-PBPM can be calculated with changing the  $D$ - and  $E$ -values. As seen in Figure 3, the greater slanting angles feature among the Z, X, and Y canonical orientations of *m*-PBPM, termed a  $D$ -gradient effect for the Z orientation and an  $E$ -gradient one for the X and Y orientations. The gradient method is facile and useful for extracting reliable spin Hamiltonian parameters from masked key canonical peaks in the frozen-glass FS ESR spectra. The procedure does not require additional empirical or phenomenological variables for the line shape analysis.

**3.2. Origins of the Line-Broadening in the FS Spectrum from *m*-PBPM in the Organic Glass: Structural Variations at the Divalent Carbons.** We have noted that the present gradient method is based on the spin Hamiltonian and a "phenomenological" approach, which is free from particular

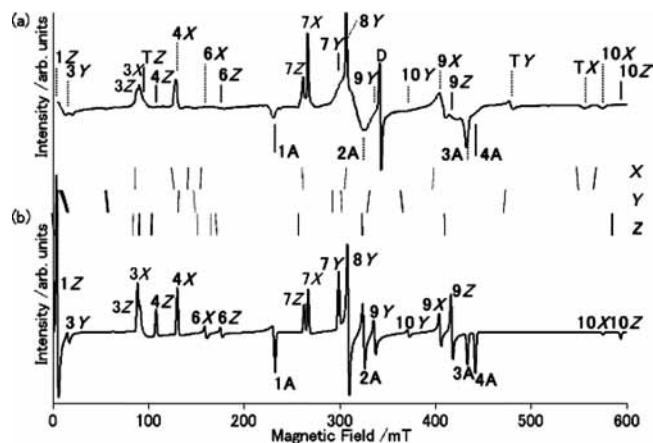


**Figure 3.** X-band FS ESR spectra of *m*-PBPM in the 2-MTHF glass. (a) Observed spectrum at 2.7 K and transition assignments. The symbols X, Y, Z denote the canonical peaks of *m*-PBPM. The symbol A denotes an off-principal-axis extra line. The bold characters designate prominently broadened lines. D at 343.37 mT denotes the signal from the doublet byproduct and T those of the phenylmethylene-based triplet carbene as the byproduct. The experimental conditions were as follows: MW frequency, 9.631 490 4 GHz; MW power, 0.2 mW; modulation frequency, 100 kHz; modulation amplitude, 0.49 mT. (b) Simulated spectrum with the Boltzmann factor considered. The spectral assignments X, Y, Z, and A denote the canonical peaks and an off-principal-axis extra line, respectively. The symbols X, Y, and Z correspond to the magnetic field orientation along the principal axis of the **D** tensor. The *m*-phenylene-based triplet species generated during the photolysis and the doublet peak (343.37 mT) as the reaction byproduct are denoted by T and D, respectively. Theoretically, 30 canonical peaks should be analytically obtained. In the perpendicular excitation spectrum, the number of the assignable canonical peaks is 26. 1X, 2X and 1Y, 2Y with imaginary resonance fields are omitted. The spectral transition assignments referred to the sublevels of *M<sub>s</sub>*, and the corresponding transition probability are given in Table S2 (Supporting Information). The broadened and diffused peaks of the quintet and triplet (T) peaks are denoted by the bold characters. The solid slanting sticks (undergoing dominant *D*-gradient effects,  $\partial B/\partial D > \partial B/\partial E$ ) and dotted ones (undergoing dominant *E*-gradient effects,  $\partial B/\partial E > \partial B/\partial D$ ) are given in the area between (a) and (b). The larger slanting angles designate the greater gradient effects, giving rise to prominent line-broadening, if the corresponding principal axes of the FS **D** tensor undergo any spatial fluctuations. The relatively sharp peaks, 7Z and 7X, are less influenced by the *D/E*-gradient effect, which are depicted by the thin and straight sticks. The detailed numerical values of  $\partial B/\partial D$  and  $\partial B/\partial E$  are given in Table S2 (Supporting Information).

chemical entities, but if the system under study undergoes any anisotropic variations of the **D** tensor, the variations will show up via the *D*- and/or *E*-gradient. Once the spin Hamiltonian parameters are determined, any gradient effects are predictable. This is the most distinguishable point compared to other phenomenological approaches to the analyses for ESR line-broadening. Any origins can be microscopic. In *m*-PBPM, both the bond angle of the divalent carbons and the dihedral angles between the central *m*-phenylene and the side phenyl ring undergo significant variation in the 2-MTHF glass compared with *m*-PBPM in the benzophenone lattice. The *D*-gradient effect is more prominent in *m*-PBPM in the glass. More relaxed molecular structures than those in the benzophenone lattice and structural variations of the parent diazo precursor in the glass or those associated with the liberation of nitrogen molecules during the photolysis at liquid helium temperature can be responsible for the microscopic origins. To determine the molecular structure of *m*-PBPM in the glass, in this study we have carried out a well-established semiempirical calculation<sup>5</sup> to evaluate the quintet **D** tensor. On the other hand, a theoretical study of significant influence of the liberation of nitrogen

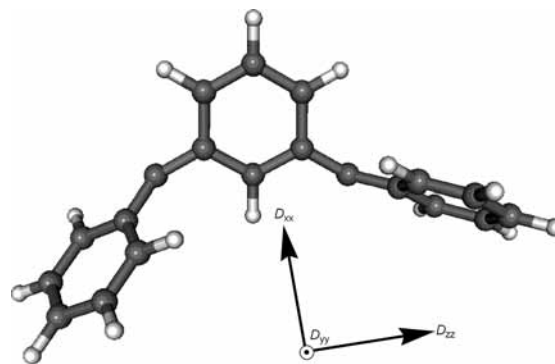


**Figure 4.** Relaxed molecular structure of *m*-PBPM in the 2-MTHF glass and the principal axes of the quintet **D** tensor. The directions of the principal values are depicted so the axes *D<sub>xx</sub>* and *D<sub>zz</sub>* lie in the sheet of the plane and the *D<sub>yy</sub>* axis is perpendicular to the plane. The proposed molecular structure of *m*-PBPM in the 2-MTHF glass is obtained in terms of the semiempirical **D**-tensor calculation.

molecules on the **D** tensor is underway in terms of more sophisticated quantum chemical calculations.

The semiempirical approach<sup>5</sup> satisfactorily reproduced both the larger *D*-value and the smaller *E/D* value for *m*-PBPM in the 2-MTHF glass, revealing that the bond angle of the divalent carbons is 5.3° larger than that constrained in the benzophenone lattice. The two dihedral angles in the glass differ by −3.1° and +3.3° (larger twisting angles with respect to the central *m*-phenylene ring), indicating the possible occurrence of a nonrelaxed molecular structure of *m*-PBPM in the benzophenone lattice. It is suggested that *m*-PBPM with a *cis*–*trans* configuration of the side phenyl ring is in a relaxed molecular structure with the larger divalent-carbon bond angle: A more “linear” structure occurs in the 2-MTHF glass,<sup>16</sup> as depicted in Figure 4 with the principal axes of the quintet **D** tensor. Notably, the derived molecular structure in the glass reminds us of Skell’s linear structure for triplet diphenylmethylene with the bond angle of 180°.

### 3.3. Generality of the Gradient Method: Application to the First Quintet *m*-Dinitrene in an Organic Glass: Structural Variations at the Nitrene Sites without Dangling Phenyl Rings.

To check the generality of the gradient method, we have applied it to the line-broadened FS spectrum of the first quintet dinitrene, *m*-phenylenebis(nitrene) (abbreviated to *m*-PBN) observed in the 2-MTHF glass.<sup>2b,4b,17</sup> The documented FS spectrum undergoes both *D*- and *E*-gradient effects, the latter being prominent, as seen in the simulated FS spectrum (see Figure S5 and Table S3 in the Supporting Information). *m*-PBN does not have dangling side phenyl rings at the divalent nitrene sites. Thus, the structural variation influential in the *D*- and/or *E*-gradient cannot arise from peripheral functional groups of *m*-PBN in its ground state. The positions of the liberated nitrogen molecules from the diazide precursor are significantly influential in the **D**-tensor variation within a certain distance from the nitrene sites.<sup>18</sup> The corrected FS parameters for the quintet dinitrene are in good harmony with the putative electronic and molecular structure at the nitrene site.<sup>17</sup> Quantum chemical calculations of high levels for the **D**-tensor fluctuations, in which the liberated nitrogen molecules located at the nitrene sites are incorporated, are underway and will be published elsewhere.

## Conclusion

In high-spin chemistry, random-orientation ESR spectroscopy is a facile and powerful method to derive spin Hamiltonian parameters of high-spin entities in frozen glasses. Seemingly

random-orientation fine-structure (FS) spectroscopy has been well established since FS ESR spectroscopy in organic glasses appeared in 1967. We have noted that the first attempt to detect the organic quintet species, *m*-PBPM, in an organic glass can date back to 1963.<sup>2c</sup> In high-spin chemistry, however, the line-broadening has been an obstacle that masks key FS transitions in many cases. Thus, both the origin of the broadening and the comprehensive spectral analysis have been a long-standing issue. In this work, we examined the origin of the line-broadening appearing in the FS ESR spectra, illustrating the comprehensive spectral analysis for the first quintet organic entity, *m*-PBPM in the quintet ground state and the first-documented quintet-state dinitrene, *m*-phenylenebis(nitrene) (*m*-PBN) in the 2-MTHF glass. A complete analysis of the random-orientation FS spectra from *m*-PBPM diluted in the benzophenone crystal has shown that the *g*-anisotropy of *m*-PBPM is not prominent and that the higher-order FS terms such as the  $S_z^2 S_y^2$  group theoretically allowed for  $S = 2$  are not necessary in spite of the argument for a hydrocarbon-based tetradical ( $S = 2$ ) in the ground state. Our new approach to analyze the FS ESR spectra undergoing the line-broadening invokes both exact analytical solutions for the resonance fields of canonical peaks and the magnetic-parameters gradient method. The *D*- and *E*-values of *m*-PBPM acquired by the spectral simulation in this study give us differences in the molecular structure of the quintet *m*-PBPM in the benzophenone crystal lattice and in the 2-MTHF glass. Microscopic origins of the line-broadening observed for high-spin oligocarbenes or oligonitrenes generated by photolysis in organic glasses have been proposed.

**Acknowledgment.** The other authors dedicate this work to the memory of the late Professor Koichi Itoh, mentor, scholar, friend. He initiated high-spin chemistry, introducing topological symmetry rules for spin alignment in organic  $\pi$ -electron network systems and organic ferromagnetism based on topologically-degenerate flat bands. This work has been supported by Grants-in-Aid for Scientific Research from the Ministry of Education, Science, Sports and Culture, Japan.

**Supporting Information Available:** Comprehensive fine-structure ESR spectral analyses including all the angular dependences of the resonance fields with the transition intensities for *m*-PBPM and *m*-PBN in the 2-MTHF glass and for the polycrystalline sample of *m*-PBPM diluted in the benzophenone crystal, the exact analytical expressions for the canonical peaks for  $S = 2$  and  $S = 1$ , and the numerical data of the gradient analyses. This material is available free of charge via the Internet at <http://pubs.acs.org>.

## References and Notes

(1) (a) *Magnetic Properties of Organic Materials*; Lahti, P. M., Ed.; Marcel Dekker: New York, 1999; Chapter 11, pp 197–236. (b) Itoh, K.,

Kinoshita, M., Eds. *Molecular Magnetism: New Magnetic Materials*; Kodansha and Gordon & Breach: Tokyo and Amsterdam, 2000. (c) *EPR of Free Radicals in Solids. Trends in Methods and Applications*; Lund, A., Shiotani, M., Eds.; Kluwer Academic Publishers: Dordrecht/Boston/London, 2003; Chapter 11, pp 407–490 and Chapter 12, pp 491–528. (d) Itoh, K.; Takui, T.; Teki, Y.; Kinoshita, T. *J. Mol. Electronics* **1988**, *4*, 181–186. (e) Itoh, K.; Takui, T. *Proc. Japan Acad., Ser. B* **2004**, *80*, 29–40.

(2) (a) Itoh, K. *Chem. Phys. Lett.* **1967**, *1*, 235–238. (b) Wasserman, E.; Murray, R. W.; Yager, W. A.; Trozzolo, A. M.; Smolinsky, G. *J. Am. Chem. Soc.* **1967**, *89*, 5076–5078. (c) Trozzolo, A. M.; Murray, R. W.; Smolinsky, G.; Yager, W. A.; Wasserman, E. *J. Am. Chem. Soc.* **1963**, *85*, 2526–2528.

(3) Wasserman, E.; Snyder, L. C.; Yager, W. A. *J. Chem. Phys.* **1964**, *41*, 1763–1772.

(4) (a) Chapyshev, S. V.; Walton, R.; Sanborn, J. A.; Lahti, P. M. *J. Am. Chem. Soc.* **2000**, *122*, 1580–1588. (b) Murata, S.; Iwamura, H. *J. Am. Chem. Soc.* **1991**, *113*, 5547–5556. (c) Chapyshev, S. V.; Tomioka, H. *Bull. Chem. Soc. Jpn.* **2003**, *76*, 2075–2089. (d) Kalgutkar, R. S.; Lahti, P. M. *Tetrahedron Lett.* **2003**, *44*, 2625–2628. (e) Ichimura, A. S.; Sato, K.; Kinoshita, T.; Takui, T.; Itoh, K.; Lahti, P. M. *Mol. Cryst. Liq. Cryst. Sect A* **1995**, *272*, 57–66.

(5) (a) Teki, Y.; Takui, T.; Itoh, K.; Iwamura, H.; Kobayashi, K. *J. Am. Chem. Soc.* **1986**, *108*, 2147–2156. (b) Teki, Y.; Fujita, I.; Takui, T.; Kinoshita, T.; Itoh, K. *J. Am. Chem. Soc.* **1994**, *116*, 11499–11505. (c) Matsushita, M.; Momose, T.; Shida, T.; Teki, Y.; Takui, T.; Itoh, K. *J. Am. Chem. Soc.* **1990**, *112*, 4700–4702. (d) Matsushita, M.; Nakamura, T.; Momose, T.; Shida, T.; Teki, Y.; Kinoshita, T.; Takui, T.; Itoh, K. *J. Am. Chem. Soc.* **1992**, *114*, 7470–7475. (e) Matsushita, M.; Nakamura, T.; Momose, T.; Shida, T.; Teki, Y.; Takui, T.; Kinoshita, T.; Itoh, K. *Bull. Chem. Soc. Jpn.* **1993**, *66*, 1333–1342. (f) Nakamura, T.; Momose, T.; Shida, T.; Kinoshita, T.; Takui, T.; Teki, Y.; Itoh, K. *J. Am. Chem. Soc.* **1995**, *117*, 11292–11298. (g) Nakamura, T.; Momose, T.; Shida, T.; Sato, K.; Nakazawa, S.; Kinoshita, T.; Takui, T.; Itoh, K.; Okuno, T.; Izuoka, A.; Sugawara, T. *J. Am. Chem. Soc.* **1996**, *118*, 8684–8687.

(6) Sato, K. Ph.D. Thesis, Osaka City University, Osaka, 1994.

(7) (a) Stoll, S.; Schweiger, A. *J. Magn. Reson.* **2006**, *178*, 42–55. (b) Castellani, et al. *Organometallics* **1997**, *16*, 4369–4376.

(8) (a) Banwell, C. N.; Primas, H. *Mol. Phys.* **1963**, *6*, 225. (b) Belford, G. G.; Belford, R. L.; Burkhardt, J. F. *J. Magn. Reson.* **1973**, *11*, 251. (c) McGregor, K. T.; Scaringe, R. P.; Hatfield, W. E. *Mol. Phys.* **1975**, *30*, 1925.

(9) Teki, Y.; Takui, T.; Yagi, H.; Itoh, K.; Iwamura, H. *J. Chem. Phys.* **1985**, *83*, 539–547.

(10) Adam, W.; van Barneveld, C.; Bottle, S. E.; Engert, H.; Hanson, G. R.; Harrer, H. M.; Heim, C.; Nau, W. M.; Wang, D. *J. Am. Chem. Soc.* **1996**, *118*, 3974–3975.

(11) Takui, T. Ph.D. Thesis, Osaka University, Osaka, 1973.

(12) Kinoshita, A.; Kubo, M.; Sugimoto, H.; Ogura, T.; Sato, K.; Takui, T.; Itoh, S. *J. Am. Chem. Soc.* **2009**, *131*, 2788–2789.

(13) Also, we have analyzed the spin Hamiltonian parameters for the diphenylmethlene-based monocarbene byproduct generated during the photolysis:  $S = 1$ ,  $g = 2.003$ ,  $D = +0.4125 \text{ cm}^{-1}$ ,  $E = -0.0195 \text{ cm}^{-1}$ .

(14)  $S = 2$ ,  $D = +0.0701 \text{ cm}^{-1}$ ,  $|E| = 0.020 \pm 0.002 \text{ cm}^{-1}$  from ref 2b.

(15) The line width was 2.0 mT for the single transition for the spectral simulation of *m*-PBPM in the 2-MTHF glass.

(16) This is also the case for the diphenylene-based monocarbene.

(17) (a) Fukuzawa, T. A. M. S. Thesis, Osaka City University, Osaka, 1994. (b) Fukuzawa, T. A.; Sato, K.; Ichimura, A. S.; Kinoshita, T.; Takui, T.; Itoh, K.; Lahti, P. M. *Mol. Cryst. Liq. Cryst. Sect A* **1996**, *278*, 253–260. (c) Chapyshev, S. V.; Walton, R.; Serwinski, P. R.; Lahti, P. M. *J. Phys. Chem. A* **2004**, *108*, 6643–6649.

(18) Anisotropic solvation of 2-MTHF in the vicinity of the nitrene sites cannot be ruled out. However, the liberated nitrogen molecules located nearest the nitrene sites are the most influential in the anisotropic line-broadening in the FS spectrum.

JP9042717